Effect of an "Ionic Liquid" Cation, 1-Butyl-3-methylimidazolium, on the Molecular Organization of H_2O

Kumiko Miki,[#,†,‡] Peter Westh,[†] Keiko Nishikawa,[§] and Yoshikata Koga*[,‡]

Department of Liberal Arts and Basic Sciences, College of Industrial Technology, Nihon University, Narashino, Chiba 275-8575, Japan, Department of Life Science and Chemistry, Roskilde University, Roskilde DK-4000, Denmark, Department of Diversity Sciences, Graduate School of Science and Technology, Chiba University, Chiba 263-8522, Japan, and Department of Chemistry, The University of British Columbia, Vancouver, B.C., Canada V6T 1Z1

Received: August 16, 2004; In Final Form: March 9, 2005

The excess partial molar enthalpy of 1-propanol (1P), H^E_{1P}, was measured at 28 °C in the ternary mixture of 1P−1-butyl-3-methylimidazolium chloride ([bmim]Cl)−H_2O in the H_2O-rich composition range. From these data we evaluated what we call the 1P−1P enthalpic interaction function, H^E_{1P-1P}. Its changes induced by addition of [bmim]Cl of the pattern of H^E_{1P-1P} were used as a probe to elucidate the effect of [bmim]Cl on the molecular organization of H_2O. It was found that the effect of Cl^- was not conspicuous within this methodology, and the observed dependence is predominantly due to the hydration of $[bmim]^+$. The changes in the x_{1P}-dependence of H^E_{1P-1P} were compared with those brought about by temperature increase, or by the addition of fructose or glycerol. It was found that the effect of $[bmim]^+$ is similar to that of fructose or increased temperature. We speculate that in the H_2O-rich composition region a number of H_2O molecules are attracted to the delocalized positive charge of the imidazolium ring and the bulk of H_2O is influenced in such a manner that the global hydrogen bond probability is reduced.

Introduction

The recent surge of interest in ionic liquids (abbreviated as IL)[1−17] is impressive due in part to their potential for greener solvents in chemical industries. In addition to chemical assessments of IL for suitability as various reaction media, their physical properties have been collected for use in process design, and of course academic interests as to why their melting points are low. ILs are generally miscible with H_2O, being ionic compounds. However, they could be designed to be made hydrophobic by choice of anion species. Even these hydrophobic ILs also tend to be hygroscopic and absorb moisture on prolonged exposure to air up to a few percent, or of the order of 0.1 mol fraction of H_2O.[7−10] The presence of H_2O, however, changes dynamic properties, viscosity in particular. It may also affect the chemistry involved as solvents, in that the reaction rate may be influenced not only by reducing bulk viscosity but also by contaminating catalytic active sites when catalysts are used. Because of this propensity, the effects of H_2O on ILs have been studied extensively of late by various modern spectroscopic techniques.[7−10] In terms of solution chemistry, however, the majority of these studies have paid attention to the H_2O-poor or the IL-rich composition region.

With this in mind, we have recently conducted a thermodynamic study on aqueous solutions of the ionic liquids 1-butyl-3-methylimidazolium ($[bmim]^+$) tetrafluoride and iodide in the entire composition range.[18] We provided three levels of thermodynamic data with an increasing order of derivative of the Gibbs energy of the system. We thus demonstrated the power of the third derivative quantities in providing more detailed information about the molecular level understanding of the mixture. We suggested that it is only below the mole fraction of IL, x_{IL}, of 0.013 to 0.015 that $[bmim]^+$ and the counteranion seem completely dissociated. At higher mole fractions than this threshold, ions begin to interact with each other and organize themselves by mutual attraction. At still higher concentration, $x_{IL} > 0.5$ to 0.6, IL molecules form clusters as in the pure state and H_2O interact with IL clusters without forming a hydrogen bond network among themselves.[18] These detailed mixing schemes, or "solution structure", were deduced by determining up to third derivatives of Gibbs energy, G. The mixing scheme described above for the IL-rich region, $x_W < 0.5$, where x_W is the mole fraction of H_2O, is consistent with the findings by spectroscopic studies for the effect of H_2O on $[bmim]BF_4$ mentioned above. Mele et al.[16] concluded from the heteronuclear Overhauser effect that tight ion pairs, $[bmim]^+$ and BF_4^-, similar to that found in its pure state, are present in the presence of H_2O for $x_W < 0.5$. H_2O, on the other hand, forms a hydrogen bond with H on C2 of the imidazolium ring, the carbon sandwiched by two nitrogen atoms. Cammarata et al.[11] using the ATR-IR technique showed that H_2O is found between anions forming the hydrogen bond as $BF_4^-\cdots HOH\cdots BF_4^-$ in the range $x_W < 0.2$. Baker et al.[13] reached the same conclusion for $[bmim]PF_6$. Thus, in this IL-rich concentration region H_2O exists as a single molecule without forming the hydrogen bond network among themselves as in liquid H_2O. We see that the mixing schemes described above obtained from the third derivative quantities in our earlier paper[18] are consistent in the IL-rich region with conclusions by some spectroscopic stuies.

* Address correspondence to this author. Phone: (604) 822-3491. Fax: (604) 822-2847. E-mail: koga@chem.ubc.ca.
[#] Nihon University.
[†] Roskilde University.
[‡] The University of British Columbia.
[§] Chiba University.

10.1021/jp046309c CCC: $30.25
Published on Web 04/13/2005

Here we limit our attention to the H_2O-rich region, in abundance of H_2O, and seek finer details of the mixing scheme in the [bmim]Cl−H_2O system, in particular how $[bmim]^+$ and Cl^- interact with H_2O. Since we have knowledge as to how Cl^- interacts with H_2O, as described below, we seek the effect of $[bmim]^+$ on the molecular organization of H_2O. We do this by applying the same methodology successful in learning the effects of various normal salts (solid at room temperature) on H_2O.[19] Namely, we study a ternary system, 1-propanol (1P)−[bmim]Cl−H_2O. We determine the third derivative thermodynamic quantity of 1P in the system and use its behavior as a probe to learn about the effect of [bmim]Cl on the molecular organization of H_2O. This methodology was successful in elucidating particularly clearly the effects of sodium salts on H_2O[19] in the Hofmeister series.[20] We showed clearly that SO_4^{2-} and SCN^-, which are placed in the opposite extremes of the Hofmeister series, modify H_2O in qualitatively different manners. Thus, the same methodology on the 1P−[bmim]Cl−H_2O system may shed some light on details of the effect of this IL cation on H_2O in the H_2O-rich region. Our interest lies in how such a large cation as $[bmim]^+$ modifies the molecular organization of H_2O.

Experimental Section

[bmim]Cl (Fluka, Buchs, Switzerland, 97.4% and H_2O content 0.6%) and 1P (Fluka, 99.8%) were used as supplied. Due care was exercised not to contaminate both chemicals further from moisture. H_2O was freshly prepared with MilliQ equipment (Millipore, Bedford, MA).

The partial molar enthalpy of 1P, H_{1P}^E, was determined by a TAM 2277 isothermal titration calorimeter (Thermometric, Jarfalla, Sweden) with a nano-Watt amplifier module. This work used a type 2250 titration module with a 1 mL stainless steel cell and a gold stirrer. The cell initially contained an aqueous solution of [bmim]Cl, into which 1P was titrated successively. The uncertainty is estimated as ± 0.03 kJ mol $^{-1}$, except for some sporadic scatter of ± 0.1 kJ mol $^{-1}$ by some unknown causes. All measurements were made at 27.98 ± 0.01 °C.

Results and Discussions

The excess partial molar enthalpy of 1P, H_{1P}^E, is the response of the system 1P−[bmim]Cl−H_2O in terms of the excess enthalpy, H^E, when the amount of 1P, n_{1P}, only is perturbed. Thus,

$$H_{1P}^E = \left(\frac{\partial H^E}{\partial n_{1P}}\right) \tag{1}$$

where the partial derivative is taken by keeping all the other variables constant, including the amounts of IL and H_2O, n_{IL} and n_W. For their measurements, the partial derivative is approximated by $(\delta H^E/\delta n_{1P})$ with $\delta n_{1P}/N < 0.01$, where $N = (n_{1P} + n_{IL} + n_W)$. This ratio was shown earlier to provide an acceptable approximation to the derivative.[21−23] As eq 1 implies, $H_{1P}{}^E$ is the actual enthalpic contribution or situation of 1P in the mixture in which complex interactions are operative among all the constituents. Hence, as argued earlier,[24−26] the following derivative H_{1P-1P}^E, a third derivative of G, signifies the effect of an additional 1P on the enthalpic situation of the existing 1P:

$$H_{1P-1P}^E \equiv N\left(\frac{\partial H_{1P}^E}{\partial n_{1P}}\right) = (1 - x_{1P})\left(\frac{\partial H_{1P}^E}{\partial x_{1P}}\right) \tag{2}$$

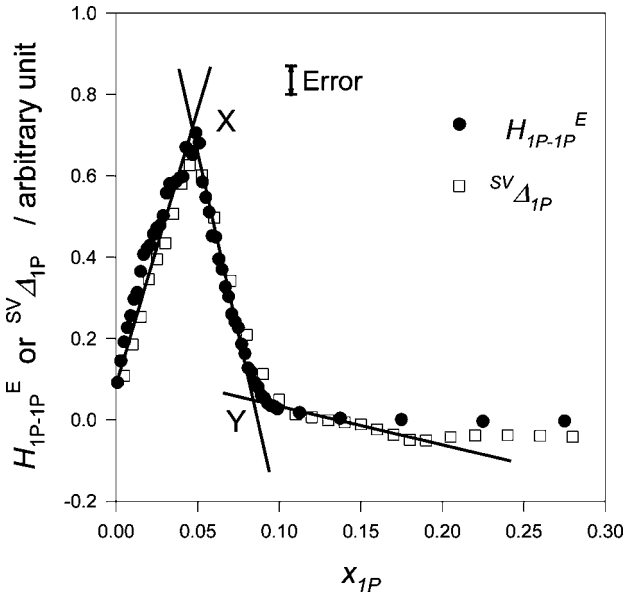

Figure 1. Enthalpic 1P−1P interaction, H_{1P-1P}^E, and the partial molar entropy−volume cross fluctuation, $^{SV}\Delta_{1P}$, in binary 1P−H_2O at 25 °C. Data from ref 32.

where x_{1P} is the mole fraction of 1P. The second equality of eq 2 provides the means to determine H_{1P-1P}^E graphically without resorting to any fitting function. The method of an acceptable approximation of graphical differentiation was discussed at some length earlier.[27] We thus have model-free, experimentally accessible information about the 1P−1P interactions.

As described earlier,[24−26,28−30] we have made an extensive study on aqueous solutions of mono-ols using these second and third derivatives of G, and elucidated mixing schemes, or "solution structures" purely from thermodynamic data, higher order derivatives of G than hitherto used. They were shown consistent with available spectroscopic studies.[24−26] We do not repeat all of our findings on binary aqueous solutions here. Briefly for 1P−H_2O, Figure 1 shows a third derivative quantity, H_{1P-1P}^E. This together with other second and third derivative quantities were used to suggest that from $x_{1P} = 0$ to point X in the figure shows the process of 1P modifying the hydrogen bond network of H_2O, while H_2O is protecting its integrity against invasion of 1P. Namely, the hydrogen bond network of H_2O is enhanced in the immediate vicinity of 1P ("iceberg formation") with concomitant reduction of the hydrogen bond probability in the bulk H_2O away from hydrophobic solutes. However, the hydrogen bond network is still connected throughout the entire bulk, i.e., the network is bond-percolated.[31] At the same time, there still exist ice-like patches in the bulk H_2O.[31,32] Thus, the integrity of liquid H_2O is retained. As the composition of 1P increases, the hydrogen bond probability of the bulk H_2O reaches a threshold value, the bond percolation threshold, at which the hydrogen bond network is no longer connected throughout the entire bulk, i.e., the bond percolation is lost. From this point onward, the solution consists of two kinds of clusters, one rich in H_2O (reminiscent of "iceberg") and the other rich in 1P (reminiscent of 1P clusters prevalent in the 1P-rich region). Point X in Figure 1 is the onset and Y the completion of the transition from the H_2O-rich mixing scheme to that in the intermediate region. As is evident from Figure 1, the loci of point X is at $x_{1P} = 0.05$ and Y at $x_{1P} = 0.09$ at 25 °C.[24−26,28−30] These conclusions are consistent with a recent X-ray diffraction study on 1P−H_2O.[33] Takamuku et al.[33] by analyzing the wide-angle X-ray scattering data from 1P−H_2O concluded that for $x_{1P} < 0.1$ the tetrahedral-like structure of H_2O (ice-like patches) is

prevalent, while for $x_{1P} > 0.1$ hydrogen bonded chains of 1P (1P-rich clusters) are present. The threshold value is approximately the same as ours. Though an X-ray diffraction aims directly at obtaining "structure", the data analysis is not free from assumptions at each of many steps of data treatment. The boundary value of x_{1P} is primarily located in their graph of "number of linear hydrogen bonds per oxygen atoms" against x_{1P}, which shows a rather blurred boundary. Furthermore the process of calculating the ordinate quantity requires one more step of integration of the pair correlation function. Considering these difficulties, the consistency with our conclusions from thermodynamic data is remarkable.

Another important point to note regarding the behavior of H^E_{1P-1P} in the binary 1P−H_2O system is that it is closely related to the fluctuation property of the system. One of us has defined the normalized entropy−volume cross fluctuation, ${}^{SV}\Delta$, together with other fluctuation functions, as,[32]

$$ {}^{SV}\Delta \equiv \langle(\Delta S/\langle V\rangle)(\Delta V/\langle V\rangle)\rangle = RT\alpha_p/V_m \qquad (3) $$

where ΔS and ΔV are the local (space/time-wise) variations from their averages $\langle S\rangle$ and $\langle V\rangle$, and V_m is the molar volume of the mixture. $\langle\ \rangle$ signifies the ensemble-average values. We showed that ${}^{SV}\Delta$ contains qualitative information about the intensity (amplitude) and the extensity (wavelength) of the entropy−volume cross fluctuation.[32] Unlike normal liquids, H_2O has a negative contribution to ${}^{SV}\Delta$ due to the putative formation/destruction of ice-like patches, i.e., coarse grains of high volume and low entropy. Hence the x_{1P}-dependence of ${}^{SV}\Delta$ reflects the process of changes in water-likeness induced by the presence of 1P. Its partial derivative with respect to the amount of 1P, ${}^{SV}\Delta_{1P}$, defined as,

$$ {}^{SV}\Delta_{1P} \equiv N\left(\frac{\partial {}^{SV}\Delta}{\partial n_{1P}}\right) = (1 - x_{1P})\left(\frac{\partial {}^{SV}\Delta}{\partial x_{1P}}\right) \qquad (4) $$

shows the effect of an additional 1P on the changes of "water-likeness" due to the presence of 1P. Figure 1 shows both plots with the scaled ordinate. As is evident in the figure, the 1P−1P enthalpic interaction and the effect of 1P on the normalized entropy−volume cross fluctuation share the same cause. We therefore suggested[24−26,32] that 1P−1P interaction is mediated via the bulk H_2O in the H_2O-rich region. While the water-likeness, a negative contribution to ${}^{SV}\Delta$, is gradually diminishing up to point X, the bulk H_2O away from 1P still maintains a characteristic fluctuation property as liquid H_2O. The upshot of all this is that the values of H^E_{1P-1P} reflect proportionally those of ${}^{SV}\Delta_{1P}$.

Here we use the x_{1P}-dependence of H^E_{1P-1P} to probe the effect of IL on H_2O in ternary 1P−[bmim]Cl−H_2O. Namely changes in the x_{1P}-dependence of H^E_{1P-1P} induced by addition of [bmim]Cl are used as a probe to elucidate the effect of IL on H_2O. This method is based on the general findings on aqueous solutions studied by us so far,[18,19,24−30] that in the H_2O-rich region the integrity of H_2O is retained though it is progressively modified by solutes. Even for multicomponent aqueous solutions, as long as the system is within the H_2O-rich mixing scheme, it is the interaction of each solute toward H_2O that dominates the molecular processes occurring in the mixture.

Figure 2 shows the plots of H^E_{1P} against x_{1P} in the mixed solvent of IL plus H_2O. x^0_{IL} is the initial mole fraction of IL in the mixed solvent. For dilute IL solutions, $x^0_{IL} < 0.01$, the x_{1P}-dependence of H^E_{1P} seems similar to that for the binary 1P−H_2O ($x^0_{IL} = 0$); the initial concave increase turns into convexity

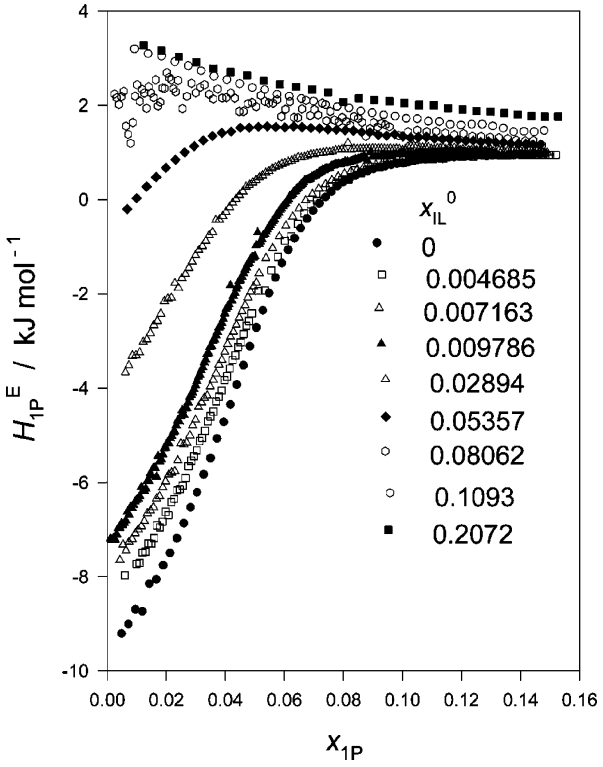

Figure 2. Excess partial molar enthalpy of 1-propanol, H^E_{1P}, at 28 °C in the mixed solvent of [bmim]Cl and H_2O at various initial concentration, x^0_{IL}. Uncertainty is estimated as ±0.03 kJ mol^{-1}, except for sporadic scatter of about ±0.1 kJ mol^{-1}. The large scatter observed for the $x^0_{IL} = 0.08$ run could be attributed to an aged microsyringe.

with an inflection point. For $x^0_{IL} > 0.03$, however, concavity is not apparent within the available data. The initial convex increase, however, remains apparent up to $x^0_{IL} = 0.082$. (The cause of wide scatter for this set of data could be attributed to an aged microsyringe used for this run.) At even higher concentration, $x^0_{IL} = 0.1$ or 0.2, no initial increase was observed. These x_{1P}-dependences of H^E_{1P} are more clearly displayed in the enthalpic interaction, H^E_{1P-1P}, eq 2. We first drew a smooth curve through all the data points of H^E_{1P} vs x_{1P}, Figure 2, using a flexible ruler, and read the data off the smooth curve drawn at intervals of 0.002 in x_{1P}. The results are listed in Table 1S, supplied as Supporting Information. Using these data, we calculated $H^E_{1P-1P} \approx (1 - x_{1P})(\delta H^E_{1P}/\delta x_{1P})$ with $\delta x_{1P} = 0.008$.[27] Results are plotted in Figure 3. The peak represents the inflection point in Figure 2 discussed above. In view of uncertainty in H^E_{1P-1P}, we located the peak by extrapolating both sides of the peak and used the intersection as point X. As mentioned above, the locus of point X marks the onset of the transition of mixing scheme from the H_2O-rich to the intermediate region in 1P−H_2O.[24−26] Namely, from $x_{1P} = 0$ to point X, the integrity of H_2O remains intact. In particular, one of the important characteristics of H_2O, that the hydrogen bond network is bond-percolated, is retained. Thus, the bond percolation nature starts to break down at point X. The x_{1P}-dependence of H^E_{1P-1P}, Figure 3, shows that on adding [bmim]Cl, the trace follows the same line up to point X and turns around to decrease at progressively smaller values of x_{1P} with a smaller value of H^E_{1P-1P}. Figure 4 shows a similar effect observed earlier for 1P−fructose−H_2O.[34]

To assess the effect of Cl^- in IL on the behavior of H^E_{1P-1P} in Figure 3, we recall our earlier similar study for 1P−NaCl−H_2O.[35] Figure 5 shows H^E_{1P-1P} in the 1P−NaCl−H_2O system.

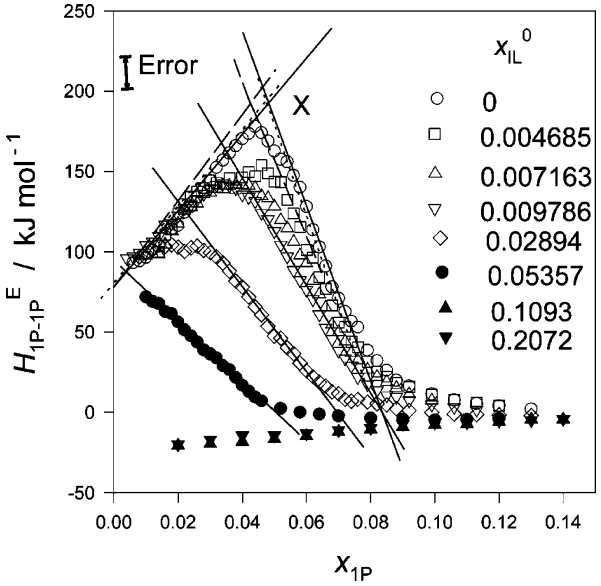

Figure 3. Enthalpic 1P−1P interaction, H^E_{1P-1P}, eq 2, in 1P−[bmim]Cl−H_2O at 28 °C. The broken line in the figure shows an estimated effect of Cl^- alone with its mole fraction $x^0_{Cl} = 0.005$. The doted line is the effect of impurities if they are hydrophobic solutes. See text.

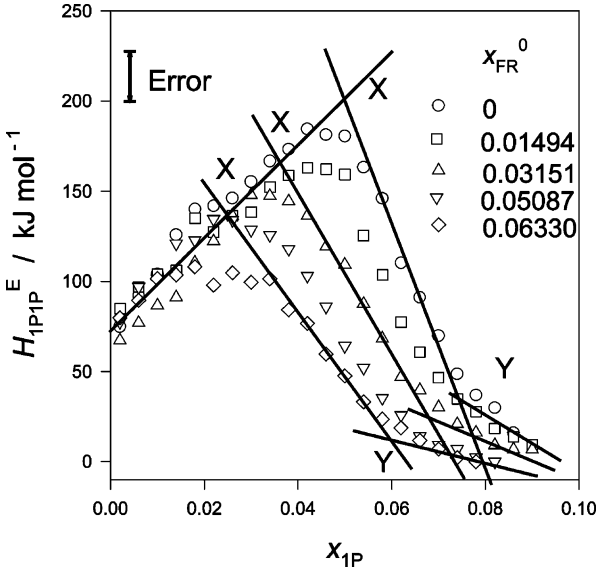

Figure 4. Enthalpic 1P−1P interaction, H^E_{1P-1P}, in 1P−fructose−H_2O at 25 °C. Data from ref 34.

The figure indicates that on addition of NaCl, point X shifts to a smaller value of x_{1P} without changing the height of the peak. At the same time the value of H^E_{1P-1P} at $x_{1P} = 0$ remains the same. These facts suggest that an NaCl hydrates a number of H_2O molecules strongly and makes them unavailable for interaction with 1P. Since the values of H^E_{1P-1P} both at $x_{1P} = 0$ and point X remain the same, the bulk H_2O away from the hydration shell appears unaltered by the presence of NaCl. From the proportionality of the shift of point X in the value of x_{1P} on increasing x^0_{NaCl}, it was estimated that an Na^+ and Cl^- ion pair hydrates 7.5 molecules of H_2O.[35] This corroborates a first principle simulation study, which concluded that a Na^+ ion hydrates 5.2 molecules of H_2O and has no effect on the bulk H_2O outside the first hydration shell.[36] It follows then that a Cl^- ion also hydrates a small number, 2, of H_2O molecules and has no effect on the bulk H_2O. It is interesting to note that an estimate of zero hydration for Cl^- was given by treating freezing

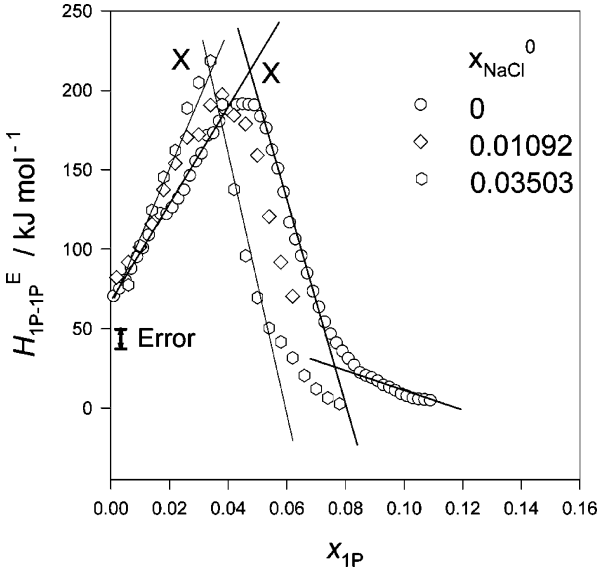

Figure 5. Enthalpic 1P−1P interaction, H^E_{1P-1P}, in 1P−NaCl−H_2O at 25 °C. Data from ref 35.

point, boiling point, vapor pressure, and osmotic pressure data of aqueous electrolytes as an ideal mixture consisting of two species H_2O and hydrated ions.[37]

As pointed out recently,[18] IL ions could be completely dissociated at a very dilute region $x_{IL} \lesssim 0.013$. The x_{1P}-dependence of H^E_{1P-1P} shown in Figure 3 has no apparent reminiscence to that from the Cl^- ion. If a Cl^- ion hydrates 2 H_2O molecules and leaves no effect on the bulk H_2O and the solution is unaffected by the countercation, the x_{1P}-dependence of H^E_{1P-1P} would look as that given by the broken line in Figure 3 for the mole fraction of Cl^-, $x^0_{Cl} = 0.05$. Thus, taking the error into consideration, we conclude what is shown in Figure 3 is predominantly the effect of the $[bmim]^+$ ion.

The [bmim]Cl specimen used here contains 0.6% of H_2O and about 2% of unidentified impurities. The 97.6% purity of [bmim]Cl and the 0.6% H_2O impurity are taken into account in calculating the initial mole fraction of IL, x^0_{IL}. The remaining 2% may most likely be unreacted methylimidazole and butyl chloride, judging from the preparation method.[38] On dissolving [bmim]Cl in H_2O up to about a half mole fraction, there was no oily phase observed. Hence we assume here that these impurities are dissolved in H_2O at present conditions, and work as hydrophobic solutes. The effects of these hydrophobic impurities on H^E_{1P-1P} would be negligible judging from our previous similar study on 1P−2-propanol (2P)−H_2O,[39] and preliminary results on 1P−2-butoxyethanol (BE)−H_2O.[40] Namely, the effect of hydrophobic 2P or BE is such that the pattern of H^E_{1P-1P} is shifted parallel to the left, or a smaller value of x_{1P} in Figure 3, proportional to the amount of 2P or BE. It follows then that 4 mol % of hydrophobic impurities in the present sample (taking the molecular weights of both impurities as a half of [bmim]Cl) will shift the H^E_{1P-1P} pattern to the left in Figure 3 by about 0.002 in x_{1P} scale, as shown by dotted lines. Hence similarly to the effect of Cl^- discussed above, the effects of impurities are negligible. What is shown in Figure 3 is therefore mainly due to $[bmim]^+$.

To elucidate the effect of [bmim] on H^E_{1P-1P}, we recall an equivalent plot in the binary aqueous *tert*-butyl alcohol (TBA) when temperature was raised.[21] Figure 6 shows the TBA−TBA enthalpic interaction, $H^E_{TBA-TBA}$, vs the mole fraction of TBA, x_{TBA}, at various temperatures. TBA shows a stronger hydro-

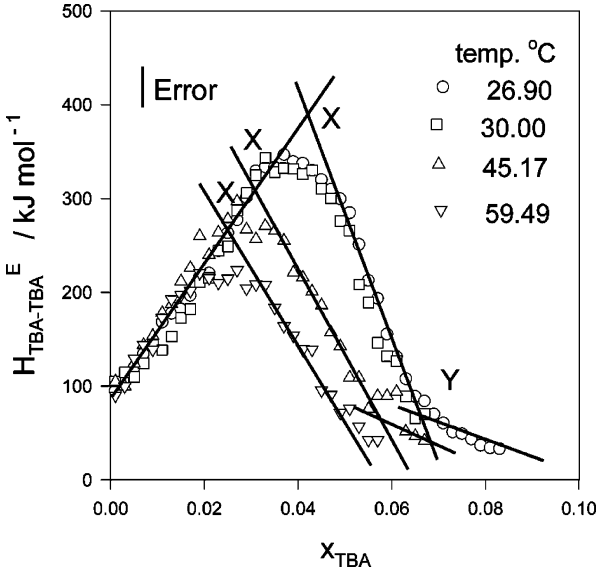

Figure 6. Enthalpic interaction between *tert*-butyl alcohol (TBA), $H^E_{TBA-TBA}$, in TBA−H_2O at various temperatures. Data from ref 21.

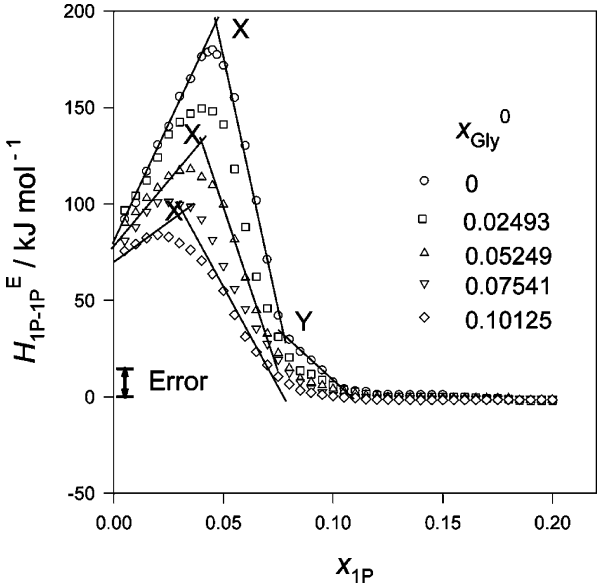

Figure 7. Enthalpic 1P−1P interaction, H^E_{1P-1P}, eq 2, in 1P−glycerol−H_2O at 25 °C. Data from ref 27.

phobic characteristics than 1P.[24−26] However, the effect of temperature on $H^E_{TBA-TBA}$ should be similar to that expected for H^E_{1P-1P}. Indeed, the same temperature dependence was also observed for the binary aqueous 2-butoxyethanol (BE),[41] which is still a stronger hydrophobic solute than TBA.[24−26] Thus, as the temperature increases, $H^E_{TBA-TBA}$ follows the same trace up to point X at progressively smaller values and then turns around to decrease as temperature increases from 26 to 60 °C. It is generally believed that the global average of the hydrogen bond probability decreases on increasing temperature.[31,32,42,43] A lower hydrogen bond probability requires a progressively lesser amount of 1P to bring the system to point X, the hydrogen bond percolation threshold. The fact that the initial trace of H^E_{1P-1P} vs x_{1P} follows the same line up to point X suggests that in the H_2O-rich region the enthalpic interaction and hence the effect of 1P on the entropy−volume cross fluctuation also remains unaffected by temperature increase although the global hydrogen bond probability is reduced.

We now compare the effects of $[bmim]^+$, Figure 3, fructose, Figure 4, and the temperature, Figure 6. An immediate and apparent conclusion from this comparison could be that the effect of $[bmim]^+$ and fructose is to reduce the global average of the hydrogen bond probability of bulk H_2O, just as temperature increase does. While it is not immediately obvious at first sight that an additive's effect could be as ubiquitous as temperature, the effect of $[bmim]^+$ or that of fructose could be of long range, perhaps via the hydrogen bond network of H_2O. The most dilute mixed solvent we used for the present study is $x^0_{IL} = 0.005$. If IL molecules are distributed randomly and H_2O molecules surround a solute molecule in a spherical fashion, the sphere contains 199 molecules ($=1/0.005-1$) of H_2O within the radius of 3.6 molecules ($=\sqrt[3]{199(3/4\pi)}$). It has been suggested that liquid H_2O is characterized by a cooperative fluctuation involving a large number of H_2O.[44−46] We showed also that the extensity (the wavelength) of fluctuations is larger than that of normal liquids.[32,42,43] If so, a few molecular distance (i.e., 3.6) may not be unreasonable for the range of interaction. We suppose for the sake of argument that such a long-range effect is operative.

Fructose contains five hydroxyl groups that are capable of forming hydrogen bonds with H_2O in addition to the ring oxygen in aqueous solution. By so doing, they could exert a long-range effect on the global hydrogen bond probability, via the hydrogen bond network inherent in H_2O. In an earlier study on the ternary 1P−glycerol−H_2O with the same methodology,[27] glycerol with three −OH groups was found to reduce the values of H^E_{1P-1P} and shifts the locus of point X to a smaller value of x_{1P}, as shown in Figure 7. From these observations we concluded that glycerol, by forming hydrogen bonds to the hydrogen bond network of H_2O, breaks the inherent H donor/acceptor symmetry. As a result, it reduces the degree of fluctuation and the average hydrogen bond probability. We suggest that some geometric differences of each species in aqueous solution may be of importance for the differences between the effect of fructose, Figure 4, and that of glycerol, Figure 7. While glycerol could be forming a dimer via alkyl backbones with 6 −OH groups pointing outward,[27] fructose is known to be in a conformation equilibrium of 5- and 6-membered rings in aqueous solutions. One of us showed earlier that the X-ray scattering data of H_2O in the range from 0 to 2.5 Å^{-1} were reproduced well by the model in which six-membered rings of the hydrogen bond network reminiscent to ice Ih connectivity are cooperatively flapping.[46] Thus there seems to be a good match in geometry between fructose and H_2O, which is lacking for glycerol or its "dimer".

Why, then, does $[bmim]^+$ modify H_2O in a similar fashon as D-fructose or temperature rise? It was shown that H on C2 between two N atoms in the imidazolium ring is capable of forming a hydrogen bond with the BF_4^- anion in the pure state.[16] When H_2O was added to $x_W = 0.09$ not only the C2 proton but H's on C4 and C5 in the imidazolium ring also form a hydrogen bond with H_2O. At even higher H_2O content, $x_W \approx 0.5$ (still a smaller H_2O content than what interests us in this paper), all the H atoms including the butyl and the methyl side chains are involve in hydrogen bonding with H_2O.[16] All these rather surprising findings must be caused or related to the delocalized charge on the imidazolium ring. In view of the resemblance of the pattern change of H^E_{1P-1P} between $[bmim]^+$ and D-fructose, and since H_2O content is much higher than 1:1 (i.e., $x_W = 0.5$), we suggest it could be the delocalized positive charge on the imidazolium five-membered ring that attracts a number of H_2O molecules with the protons of H_2O pointing outward. This hydration structure may resemble the −OH groups on fructose in aqueous solution. Clearly more examples of imidazolium ions

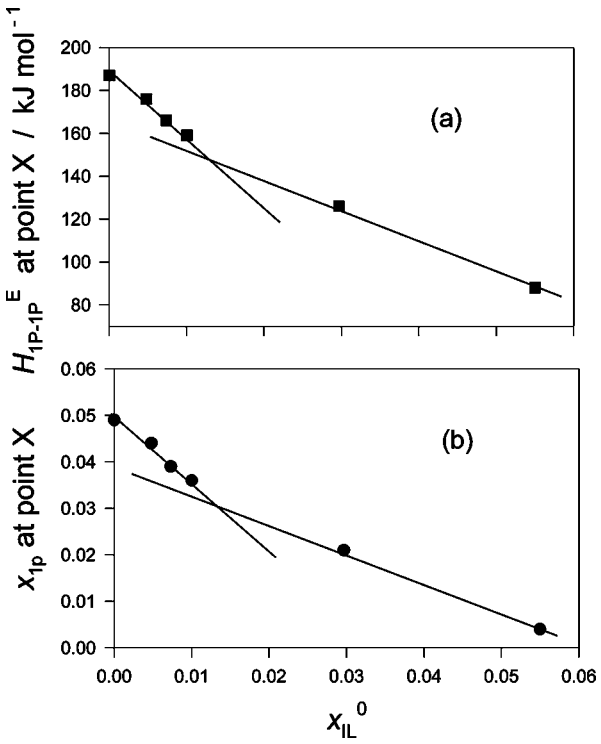

Figure 8. Loci of point X at various initial mole fractions of the mixed solvent, x^0_{IL}: (a) in terms of H^E_{1P-1P} and (b) in terms of x_{1P}.

with various hydrophobic branches ought to be gathered systematically and other experimental techniques must be applied for further elucidation of the hydration of $[bmim]^+$ in the H_2O-rich region.

Turning back to Figure 3, the behavior of H^E_{1P-1P} does not conspicuously show a qualitative change at about the earlier suggested boundary of $x^0_{IL} \approx 0.013$. To seek this more clearly, the loci of point X are plotted in Figure 8 as a function of x^0_{IL}, in terms of the values of H^E_{1P-1P} and x_{1P} at point X. While more data points are desirable, the plots could suggest two different mechanisms represented by the two straight lines, which cross at $x^0_{IL} \approx 0.013$. As pointed out earlier,[18] above this threshold, $x^0_{IL} \gtrsim 0.013$, $[bmim]^+$ and a counteranion begin to attract each other and start to organize themselves. If the effect of $[bmim]^+$ on H_2O is indeed due to the de-localized positive charge in the imidazolium ring as discussed above, the positive charges are partially masked by the counter Cl^- ion in this range. Hence the slope in Figure 8 becomes smaller (less negative) than that in the H_2O-rich region. Thus the data in Figure 8 are not inconsistent with the threshold value of about 0.013 and support a change in dissociation characteristics at this threshold suggested earlier.[18] In closing, we provided circumstantial evidence for the earlier speculation that IL ions are dissociated below a threshold, $x_{IL} \approx 0.013$, and above this composition ions start to attract each other. Furthermore, we suggest that in the H_2O-rich composition range the hydration "structure" is similar to that by D-fructose and its net effect is to reduce the hydrogen bond probability of bulk H_2O away from solutes.

Acknowledgment. We thank Nihon University, the Carlsberg Foundation, and the Danish Technical Research Council for their support.

Supporting Information Available: Table of smoothed values of excess partial molar enthalpies of 1-propanol. This material is available free of charge via the Internet at http://pubs.acs.org.

References and Notes

(1) Wasserscheim, P.; Welton, T., Eds. *Ionic Liquids in Syntheses*; VCH-Wiley, Weinheim, Germany, 2003.
(2) Jessop, P. G. *J. Synth. Org. Chem.* **2003**, *61*, 483.
(3) Welton, T. *Chem. Rev.* **1999**, *99*, 2071.
(4) Jessop, P. G.; Stanley, R. R.; Brown, R.A.; Echert, C. A.; Lietta, C. L.; Ngo, T. T.; Pollet, P. *Green Chem.* **2003**, *5*, 123.
(5) Rogers, R. D.; Seddon, K. R. Ionic Liquids—Industrial Applications for Green Chemistry; ACS Symp. Ser. 818; American Chemical Society: Washington, DC, 2002.
(6) Wasserscheim, P.; Kein, W. *Angew. Chem.* **2000**, *39*, 3772.
(7) Jessop, P. G. Private communication.
(8) Seddon, K. R.; Stark, A.; Torres, M.-J. *Pure Appl. Chem.* **2000**, *72*, 2275.
(9) Anthony, J. L.; Maginn, E. J.; Brenecke, J. F. *J. Phys. Chem. B* **2001**, *105*, 10942.
(10) Pandey, S.; Fletcher, K. A.; Baker, S. N.; Baker, G. A. *Analyst* **2004**, *129*, 569.
(11) Cammarata, L.; Kazarian, S. G.; Slater, P. A.; Welton, T. *Phys. Chem. Chem. Phys.* **2001**, *3*, 5192.
(12) Baker, S. N.; Baker, G. A.; Bright, F. V. *Green Chem.* **2002**, *4*, 165.
(13) Baker, S. N.; Baker, G. A.; Munson, C. A.; Chen, F.; Bukowski, E. J.; Cartwright, A. N.; Bright, F. V. *Ind. Eng. Chem. Res.* **2003**, *42*, 6457.
(14) Werner, J. H.; baker, S. N.; Baker, G. A. *Analyst* **2003**, *128*, 786.
(15) Fletcher, K. A.; Pandey, S. *J. Phys. Chem. B* **2003**, *107*, 13532.
(16) Mele, A.; Tran, C. D.; Lacerda, S. H. D. *Angew. Chem., Int. Ed.* **2003**, *42*, 4364.
(17) Fletcher, K. A.; Baker, S. N.; Baker, G. A.; Pandey, S. *New J. Chem.* **2003**, *27*, 1706.
(18) Katayanagi, H.; Nishikawa, K.; Shimozaki, H.; Miki, K.; Westh, P.; Koga, Y. *J. Phys. Chem. B* **2004**, *108*, 19451.
(19) Koga, Y.; Westh, P.; Davies, J. V.; Miki, K.; Nishikawa, K.; Katayanagi, H. *J. Phys. Chem. A* **2004**, *108*, 8533.
(20) Creighton, T. E. *Proteins, Structures and Molecular Properties*; 2nd ed.; W. H. Freeman: New York, 1993.
(21) Koga, Y. *Can. J. Chem.* **1988**, *66*, 1187.
(22) Koga, Y. *Can. J. Chem.* **1988**, *66*, 3171.
(23) Koga, Y. *Comprehensive Handbook of Calorimetry and Thermal Analysis;* Sorai, M., et al., Eds.; John Wiley & Sons: New York, 2004; Section 3.1.3, pp 195−199.
(24) Koga, Y. *J. Cryst. Soc. Jpn.* **1995**, *64*, 206.
(25) Koga, Y. *J. Phys. Chem.* **1996**, *100*, 5172.
(26) Koga, Y. *Netsu Sokutei* **2003**, *30*, 54. Available in pdf form on request to the author.
(27) Parsons, M. T.; Westh, P.; Davies, J. V.; Trandum. Ch.; To, E. C. H.; Chiang, W. M.; Yee, E. G. M.; Koga, Y. *J. Solution Chem.* **2001**, *30*, 1007.
(28) Tanaka, S. H.; Yoshihara, H. I.; Ho, A. W.-C.; Lau, F. W.; Westh, P.; Koga, Y. *Can. J. Chem.* **1996**, *74*, 713.
(29) Hu, J.; Haynes, C. A.; Wu, A. H. Y.; Cheung, C. M. W.; Chen, M. M.; Yee, E. G. M.; Ichioka, K.; Koga, Y. *Can. J. Chem.* **2003**, *81*, 141.
(30) Koga, Y.; Westh, P.; Nishikawa, K. *Can. J. Chem.* **2003**, *81*, 150.
(31) Stanley, H. E.; Teixeira, J. *J. Chem. Phys.* **1980**, *73*, 3404.
(32) Koga, Y. *Can. J. Chem.* **1999**, *77*, 2039.
(33) Takamuku, T.; Maruyama, H.; Watanabe, K.; Yamaguchi, T. *J. Solution Chem.* **2004**, *33*, 641.
(34) To, E. C. H.; Westh, P.; Trandum, Ch.; Hvidt, Aa.; Koga, Y. *Fluid Phase Equilib.* **2000**, *171*, 151.
(35) Matsuo, H.; To, E. C. H.; Wong, D. C. Y.; Sawamura, S.; Taniguchi, Y.; Koga, Y. *J. Phys. Chem. B* **1999**, *103*, 2981.
(36) White, J. A.; Schwegler, E.; Galli, G.; Gygi, F. *J. Chem. Phys.* **2000**, *113*, 4668.
(37) Zavitsas, A. A. *J. Phys. Chem. B* **2001**, *105*, 7805.
(38) Huddleston, J. G.; Visser, A. E.; Reichert, W. M.; Willauer, H. D.; Broker, G. A.; Rogers, R. D. *Green Chem.* **2001**, *3*, 156.
(39) Hu, J.; Chiang, W. M.-D.; Westh, P.; Chen, D. H. C.; Haynes, C. A.; Koga, Y. *Bull. Chem. Soc. Jpn.* **2001**, *74*, 809.
(40) Koga, Y. To be submitted for publication.
(41) Koga, Y.; Siu, W. W. Y.; Wong, T. Y. H. *J. Phys. Chem.* **1990**, *94*, 2028.
(42) Koga, Y.; Westh, P.; Sawamura, S.; Taniguchi, Y. *J. Chem. Phys.* **1990**, *105*, 2028.
(43) Koga, Y.; Tamura, K. *Netsu Sokutei* **2000**, *27*, 3404.
(44) Tanaka, T.; Ohmine, I. *J. Chem. Phys.* **1987**, *87*, 6128.
(45) Ohmine, I. *J. Phys. Chem.* **1995**, *99*, 6767.
(46) Iijima, T.; Nishikawa, K. *J. Chem. Phys.* **1994**, *101*, 5017.